ISSN 1070-3284, Russian Journal of Coordination Chemistry, 2019, Vol. 45, No. 5, pp. 378–384. © Pleiades Publishing, Ltd., 2019.

Synthesis, Characterization, and Crystal Structures of Oxidovanadium(V) Complexes Derived from 2-Chloro-*N*′-(3,5-Dichloro-2-Hydroxybenzylidene)benzohydrazide with Antimicrobial Activity

S. M. Wu[a], X. Y. Qiu[a], *, J. C. Wang[b], S. J. Liu[a], and L. Y. He[a]

[a]*College of Science & Technology, Ningbo University, Ningbo, 315212 P.R. China*

[b]*College of Chemistry, Chemical Engineering and Material Science, Shandong Normal University, Jinan, 250014 P.R. China*

**e-mail: xiaoyang_qiu@126.com*

Received May 1, 2018; revised July 26, 2018; accepted September 20, 2018

Abstract—Two new oxodovanadium(V) complexes, [VO(L)(OEt)(MeOH)] (**I**) and [VO(L)(Bha)] · EtOH (**II**), where L is the anion of 2-chloro-*N*′-(3,5-dichloro-2-hydroxybenzylidene)benzohydrazide (H_2L), Bha is the anion of 2-hydroxybenzohydroxamic acid (HBha), were prepared and characterized by IR, UV-Vis and single crystal X-ray determination (CIF files CCDC nos. 1840661 (**I**) and 1840662 (**II**)). Complex **I** crystallizes as the monoclinic space group $P2_1/c$ with unit cell dimensions a = 8.272(1), b = 21.326(2), c = 12.979(1) Å, β = 107.173(2)°, V = 2187.5(4) Å^3, Z = 4, R_1 = 0.0811, wR_2 = 0.2152, GOOF = 1.048. Complex **II** crystallizes as the triclinic space group $P\bar{1}$ with unit cell dimensions a = 7.407(2), b = 14.195(2), c = 14.330(2) Å, α = 117.262(2)°, β = 92.947(2)°, γ = 95.771(2)°, V = 1324.4(4) Å^3, Z = 2, R_1 = 0.0919, wR_2 = 0.1539, GOOF = 0.986. X-ray analysis indicates that the complexes are mononuclear vanadium(V) species, with the V atoms in octahedral coordination. The complexes were evaluated for their antibacterial (*Bacillus subtilis*, *Staphylococcus aureus*, *Escherichia coli*, and *Pseudomonas fluorescence*) and antifungal (*Candida albicans* and *Aspergillus niger*) activities by MTT (3-(4,5-dimethylthiazol-2-yl)-2,5-diphenyl tetrazolium bromide) method. The two complexes have from medium to strong activities against *B. subtilis*, *S. aureus*, and *E. coli*.

Keywords: hydrazone, vanadium complex, mononuclear complex, crystal structure, antimicrobial activity

DOI: 10.1134/S1070328419040109

INTRODUCTION

Hydrazones containing CH=N–NH–C(O) group are a kind of biological active compound. The compounds have attracted remarkable attention for their wide range of biological activities, such as antibacterial [1–3], antifungal [4, 5], and antitumor [6, 7]. It was reported that hydrazones bearing electron-withdrawing groups can improve their antimicrobial activities [8, 9]. Rai and co-workers reported a series of fluoro, chloro, bromo, and iodo-substituted compounds, and found that they have significant antimicrobial activities [10]. Vanadium complexes with Schiff bases and hydrazones have been reported to have interesting antibacterial activities [11–14]. As a continuation of work on the exploration of novel complex based antimicrobial agents, in this paper, two new oxodovanadium(V) complexes, [VO(L)(OEt)-(MeOH)] (**I**) and [VO(L)(Bha)] · EtOH (**II**), where L is the anion of 2-chloro-N'-(3,5-dichloro-2-hydroxybenzylidene)benzohydrazide (H_2L), Bha is the anion of 2-hydroxybenzohydroxamic acid (HBha), have been presented.

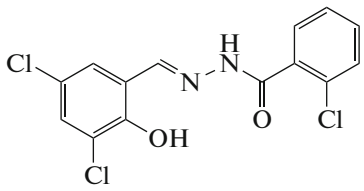

(H_2L)

EXPERIMENTAL

Materials and methods. Vanadyl acetylacetonate and organic materials were purchased from Sigma-Aldrich and used as received. All other reagents were of analytical reagent grade. Elemental analyses of C, H, and N were carried out in a Perkin-Elmer automated model 2400 Series II CHNS/O analyzer. FT-IR spectra were obtained on a Perkin-Elmer 377 FT-IR spectrometer with samples prepared as KBr pellets. UV-Vis spectra were obtained on a Lambda 900 spectrometer. ^{1}H NMR data were recorded on a

Bruker 300 MHz spectrometer. X-ray diffraction was carried out on a Bruker APEX II CCD diffractometer.

Synthesis of H_2L. To the methanolic solution (30 mL) of 2-chlorobenzohydrazide (0.01 mol, 1.70 g) was added a methanolic solution (30 mL) of 3,5-dichlorosalicylaldehyde (0.01 mol, 1.90 g) with stirring. The mixture was stirred for 30 min at room temperature, and left to slowly evaporate to give crystalline product, which were obtained by filtration. The yield was 92%.

IR data (ν, cm^{-1}): 3455 (OH), 3323 (NH), 1657 (C=O), 1602 (C=N). UV-Vis data (MeOH; λ_{max}, nm): 295, 332. ^1H NMR (300 MHz; d^6-DMSO; δ, ppm): 12.52 (s., 1H, O*H*), 12.39 (s., 1H, N*H*), 8.56 (s., 1H, C*H*=N), 7.69–7.60 (m., 2H, Ar*H*), 7.55–7.37 (m., 4H, Ar*H*).

For $C_{14}H_9N_2O_2Cl_3$

Anal. calcd., %	C, 48.94	H, 2.64	N, 8.15
Found, %	C, 49.17	H, 2.75	N, 8.06

Synthesis of complex I. H_2L (1.0 mmol, 0.343 g) and vanadyl acetylacetonate (1.0 mmol, 0.265 g) were mixed in a mixture of methanol (30 mL) and ethanol (20 mL). The mixture was refluxed for 1 h and then cooled to room temperature. Single crystals of the complex, suitable for X-ray diffraction, were formed upon slowly evaporation within a few days. The crystals were isolated by filtration. The yield was 38%.

IR data (ν, cm^{-1}): 3387 (OH), 1605 (C=N), 949 (V=O). UV-Vis data (CH_3CN; λ_{max}, nm): 260, 325, 407. ^1H NMR (300 MHz; d^6-DMSO; δ, ppm): 8.91 (s., 1H, C*H*=N), 7.83 (d., 1H, Ar*H*), 7.55–7.38 (m., 5H, Ar*H*), 3.46 (q., 2H, OCH_2CH_3), 3.35 (s., 3H, CH_3OH), 1.07 (t., 3H, OCH_2CH_3).

For $C_{17}H_{16}N_2O_5Cl_3V$

Anal. calcd., %	C, 42.05	H, 3.32	N, 5.77
Found, %	C, 42.23	H, 3.43	N, 5.66

Synthesis of complex II. Complex **I** (0.1 mmol, 48.6 mg) and 2-hydroxybenzohydroxamic acid (0.1 mmol, 15.3 mg) were mixed in ethanol (15 mL). The mixture was refluxed for 30 min and then cooled to room temperature. Single crystals of the complex, suitable for X-ray diffraction, were formed upon slowly evaporation within a few days. The crystals were isolated by filtration. The yield was 57%.

IR data (ν, cm^{-1}): 3392 (OH), 3217 (NH), 1641 (C=O), 1605 (C=N), 950 (V=O). UV-Vis data (CH_3CN; λ_{max}, nm): 255, 333, 410. ^1H NMR (300 MHz; d^6-DMSO; δ, ppm): 12.17 (s., 1H, O*H*), 8.91 (s., 1H, C*H*=N), 7.92 (d., 1H, Ar*H*), 7.83 (d., 1H, Ar*H*), 7.55–7.38 (m., 6H, Ar*H*), 7.25 (t., 1H, Ar*H*), 6.83 (d., 1H, Ar*H*).

For $C_{23}H_{19}N_3O_7Cl_3V$

Anal. calcd., %	C, 45.53	H, 3.16	N, 6.93
Found, %	C, 45.67	H, 3.05	N, 7.10

X-ray crystallography. X-ray diffraction was carried out at a Bruker APEX II CCD area diffractometer equipped with MoK_α radiation (λ = 0.71073 Å). The collected data were reduced with SAINT [15], and multi-scan absorption correction was performed using SADABS [16]. The structures of the complexes were solved by direct method, and refined against F^2 by full-matrix least-squares method using SHELXTL [17]. All of the non-hydrogen atoms were refined anisotropically. The methanol hydrogen in **I** and amino hydrogen atom in **II** were located from electronic density maps and refined isotropically. The remaining hydrogen atoms were placed in calculated positions and constrained to ride on their parent atoms. The crystallographic data and refinement parameters for the compounds are listed in Table 1. Selected bond lengths and angles are listed in Table 2.

Supplementary material for structures has been deposited with the Cambridge Crystallographic Data Centre (CCDC nos. 1840661 (**I**) and 1840662 (**II**); deposit@ccdc.cam.ac.uk or http://www.ccdc.cam.ac.uk).

Antimicrobial assay. The antibacterial activities of the free hydrazone compound and the complexes were tested against *B. subtilis*, *S. aureus*, *E. coli*, and *P. fluorescence* using MH (Mueller–Hinton) medium. The antifungal activities of the compounds were tested against *C. albicans* and *A. niger* using RPMI-1640 medium. The MIC values of the tested compounds were determined by a colorimetric method using the dye MTT [18]. A stock solution of the compound (150 μg mL^{-1}) in DMSO was prepared and graded quantities (75, 37.5, 18.8, 9.4, 4.7, 2.3, 1.2, 0.59 μg mL^{-1}) were incorporated in specified quantity of the corresponding sterilized liquid medium. A specified quantity of the medium containing the compound was poured into micro-titration plates. Suspension of the microorganism was prepared to contain approximately 1.0×10^5 cfu mL^{-1} and applied to microtitration plates with serially diluted compounds in DMSO to be tested and incubated at 37°C for 24 and 48 h for bacterial and fungi, respectively. Then the MIC values were visually determined on each of the microtitration plates, 50 μL of PBS (phosphate buffered saline 0.01 mol L^{-1}, pH 7.4) containing 2 mg of MTT mL^{-1} was added to each well. Incubation was continued at room temperature for 4–5 h. The content of each well was removed and 100 μL of isopropanol containing 5% 1 mol L^{-1} HCl was added to extract the dye. After 12 h of incubation at room temperature, the

Table 1. Crystallographic and refinement data for the complexes **I** and **II**

Complex	Value	
	I	**II**
Formula weight	485.61	606.70
Crystal shape/color	Block/brown	Block/brown
T, K	298(2)	298(2)
Crystal dimensions, mm	0.18 × 0.15 × 0.15	0.21 × 0.20 × 0.17
Crystal system	Monoclinic	Triclinic
Space group	$P2_1/c$	$P\bar{1}$
a, Å	8.272(1)	7.407(2)
b, Å	21.326(2)	14.195(2)
c, Å	12.979(1)	14.330(2)
α, deg	90	117.262(2)
β, deg	107.173(2)	92.947(2)
γ, deg	90	95.771(2)
V, Å^3	2187.5(4)	1324.4(4)
Z	4	2
ρ_{calcd}, g cm^{-3}	1.475	1.521
$\mu(MoK_\alpha)$, mm^{-1}	0.849	0.724
F(000)	984	616
Measured reflections	12725	6802
Unique reflections	4055	4639
Observed reflections ($I \geq 2\sigma(I)$)	2221	1855
Min. and max. transmission	0.8622 and 0.8833	0.8628 and 0.8868
Parameters	257	341
Restraints	3	1
Goodness of fit on F^2	1.048	0.986
R_1, wR_2 ($I \geq 2\sigma(I)$)*	0.0811, 0.2152	0.0919, 0.1539
R_1, wR_2 (all data)*	0.1427, 0.2603	0.2233, 0.2042

* $R_1 = F_o - F_c/F_o$, $wR_2 = [\sum w(F_o^2 - F_c^2)/\sum w(F_o^2)^2]^{1/2}$.

optical density was measured with a microplate reader at 550 nm.

RESULTS AND DISCUSSION

The hydrazone compound H_2L was readily prepared by the condensation reaction of 3,5-dichlorosalicylaldehyde with 2-chlorobenzohydrazide in methanol. Complex **I** was prepared by the reaction of the hydrazone compound with vanadyl acetylacetonate in methanol and ethanol. Complex **II** was prepared by reaction of complex **I** with HBha in ethanol. Complex **II** can also be prepared by the reaction of the hydrazone compound with vanadyl acetylacetonate and HBha in ethanol. Elemental analyses of the complexes are in accordance with the molecular structures proposed by the X-ray analysis.

In the spectra of the free hydrazone compound and the complexes, the weak and broad bands centered at about 3400 cm^{-1} are assigned to the vibration of O–H bonds. The weak and sharp bands located at 3323 cm^{-1} of the free hydrazone compound and 3217 cm^{-1} of complex **II** are assigned to the vibration of N–H bonds. The intense bands at 1657 cm^{-1} of H_2L and 1641 cm^{-1} of complex **II** are generated by ν(C=O) vibrations, whereas the bands at 1602–1606 cm^{-1} by the ν(C=N) ones. The non-observation of the ν(C=O) bands, present in the spectrum of the hydrazone compounds, indicates the enolization of the amide functionality upon coordination to the V-center. Instead strong bands at 1605 cm^{-1} for the complexes are observed, which can be attributed to the asymmetric stretching vibration of the conjugated CH=N–N=C–O groups,

Table 2. Selected bond distances (Å) and angles (deg) for the complexes **I** and **II**

Bond	*d*, Å	Bond	*d*, Å
		I	
V(1)–O(1)	1.869(4)	V(1)–O(2)	1.954(5)
V(1)–O(3)	1.575(5)	V(1)–O(4)	1.756(4)
V(1)–O(5)	2.324(5)	V(1)–N(1)	2.124(5)
		II	
V(1)–O(1)	1.915(6)	V(1)–O(2)	1.967(5)
V(1)–O(3)	2.244(6)	V(1)–O(4)	1.871(5)
V(1)–O(6)	1.593(5)	V(1)–N(1)	2.087(6)
Angle	ω, deg	Angle	ω, deg
		I	
O(3)V(1)O(4)	101.8(2)	O(3)V(1)O(1)	98.3(3)
O(4)V(1)O(1)	100.3(2)	O(3)V(1)O(2)	98.3(2)
O(4)V(1)O(2)	97.0(2)	O(1)V(1)O(2)	152.9(2)
O(3)V(1)N(1)	95.3(2)	O(4)V(1)N(1)	161.9(2)
O(1)V(1)N(1)	83.0(2)	O(2)V(1)N(1)	74.2(2)
O(3)V(1)O(5)	174.8(2)	O(4)V(1)O(5)	83.0(2)
O(1)V(1)O(5)	82.5(2)	O(2)V(1)O(5)	79.1(2)
N(1)V(1)O(5)	79.7(2)		
		II	
O(6)V(1)O(4)	95.0(2)	O(6)V(1)O(1)	100.0(3)
O(4)V(1)O(1)	104.7(2)	O(6)V(1)O(2)	99.9(3)
O(4)V(1)O(2)	91.5(2)	O(1)V(1)O(2)	153.1(2)
O(6)V(1)N(1)	100.0(2)	O(4)V(1)N(1)	161.2(2)
O(1)V(1)N(1)	84.0(2)	O(2)V(1)N(1)	74.8(2)
O(6)V(1)O(3)	171.2(2)	O(4)V(1)O(3)	76.2(2)
O(1)V(1)O(3)	82.8(2)	O(2)V(1)O(3)	80.3(2)
N(1)V(1)O(3)	88.6(2)		

characteristic for the coordination of the enolate form of the compounds. The strong ν(V=O) bands at 949 cm^{-1} for **I** and 950 cm^{-1} for **II** could be clearly identified for both complexes [19].

In the electronic spectra of the complexes, the lowest energy transition bands are observed at 407 nm for **I** and 410 nm for **II**, which are attributed to LMCT transition as charge transfer from *p*-orbital on the lone-pair of ligands' oxygen atoms to the empty *d*-orbital of the vanadium atoms. The other strong bands in the range of 320–340 nm in the spectra of both complexes are similar to the absorption bands in the spectra of the corresponding hydrazone compounds, so they are attributed to the intra-ligand $\pi \rightarrow \pi^*$ absorption peak of the ligands. The other mainly LMCT and to some extent $\pi \rightarrow \pi^*$ bands appear at 260 nm for **I** and 255 nm for **II**, and this is due to the oxygen donor atoms bound to vanadium(V) [19].

Molecular structure of complex **I** is shown in Fig. 1a. The coordination geometry around the vanadium atom can be described as a distorted octahedral with the tridentate hydrazone ligand coordinated in a meridional fashion, forming five- and six-membered chelate rings with bite angles of 74.2(2)° and 83.0(2)°, respectively, typical for this type of ligand systems [20]. The chelating hydrazone ligand lies in a plane with one ethanolato ligand which lies *trans* to the hydrazone imino N atom. One methanol O atom *trans* to the oxo group completes the distorted octahedral coordination sphere at a rather elongated distance of 2.324(5) Å, due to the *trans* influence of the oxo group. This is accompanied by a significant displacement of the vanadium atom from the plane defined by the four basal donor atoms towards the apical oxo oxygen atom by 0.287(2) Å. The coordinate bond lengths agree well with reported vanadium complexes containing this ligand type [20, 21]. In the crystal packing structure of the complex, hydrazone molecules are

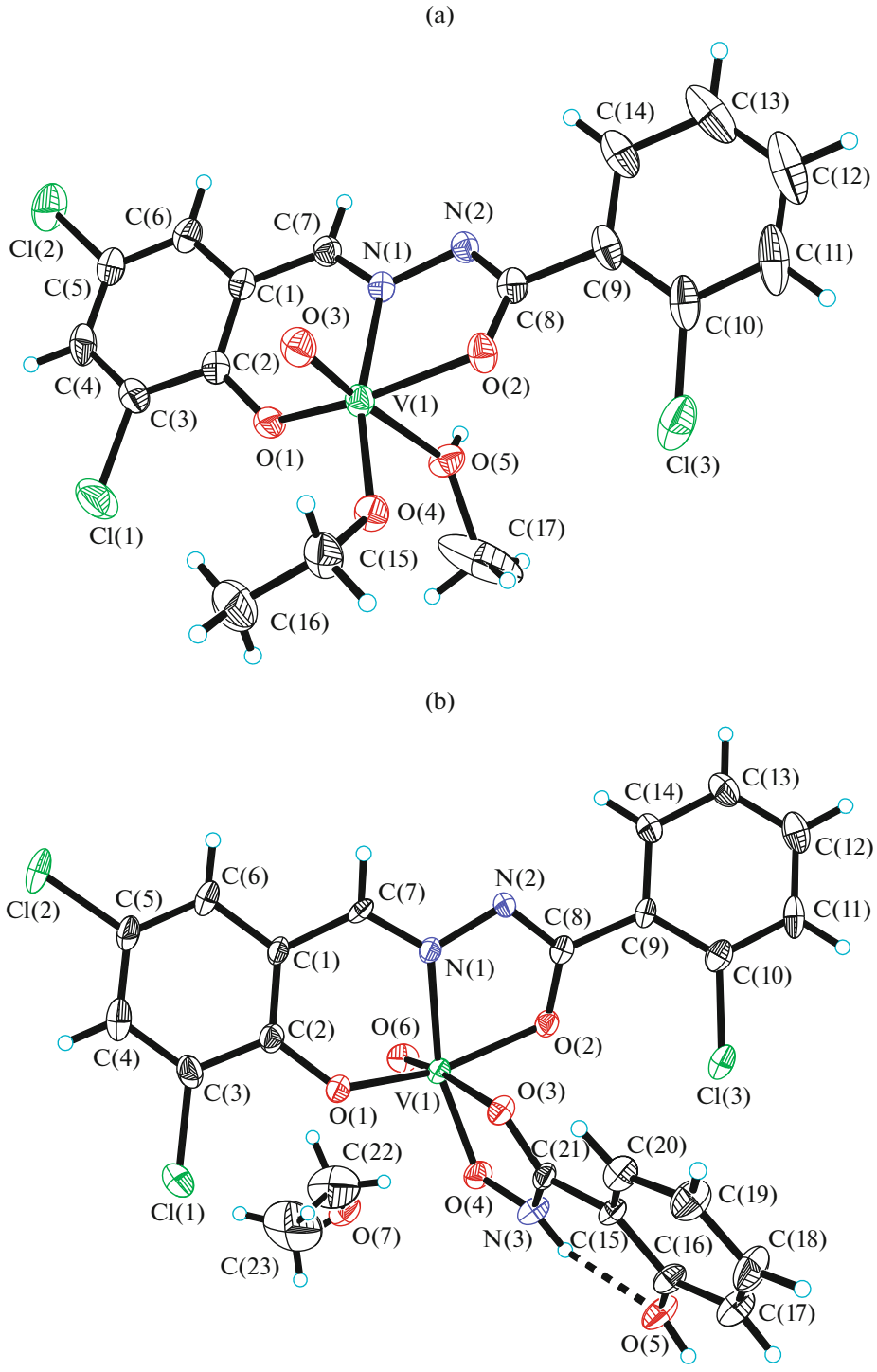

Fig. 1. A perspective view of complexes **I** (a) and **II** (b) with the atom labeling scheme. Thermal ellipsoids are drawn at the 30% probability level.

linked by methanol molecules through intermolecular hydrogen bonds of O–H···N (O(5)–H(5) 0.85(1), H(5)···N(2)^{i} 2.03(2), O(5)···N(2)^{i} 2.873(7) Å, O(5)–H(5)···N(2)^{i} 170(11)°; symmetry code for ^{i} $1-x$, $1-y$, $1-z$) to form dimers (Fig. 2a).

Molecular structure of complex **II** is shown in Fig. 1b. The asymmetric unit of the complex contains a vanadium complex molecule and an ethanol molecule of crytallization. There is an intramolecular hydrogen bond in the complex molecule (N(3)–H(3)

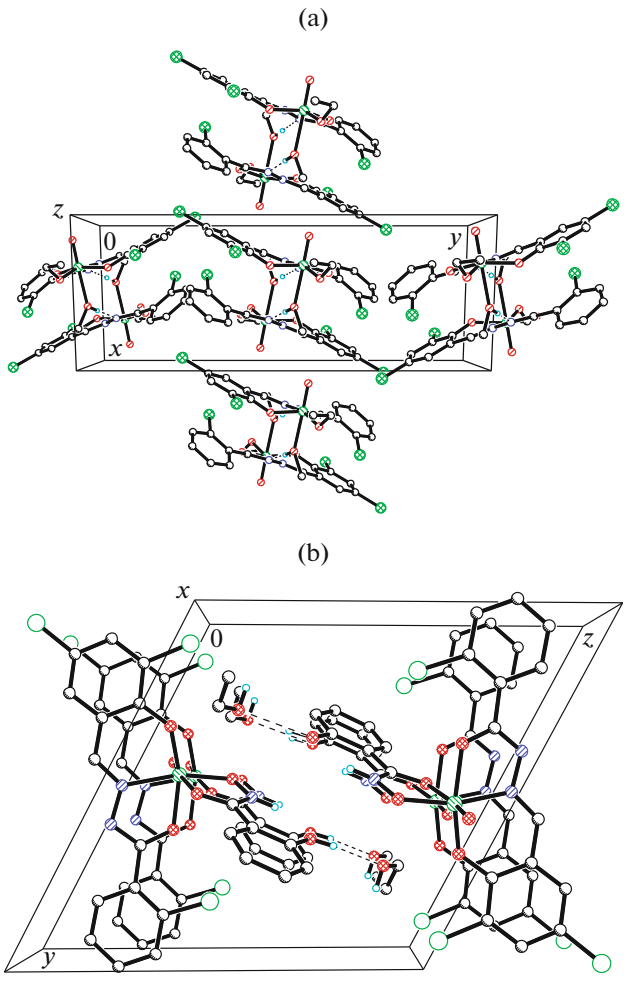

Fig. 2. Hydrogen bonds linked crystal packing structure of complex **I** (a) and **II** (b).

0.90(1), H(3)···O(5) 2.00(5), N(3)···O(5) 2.630(9) Å, N(3)–H(3)···O(5) 125(5)°). The coordination geometry around the vanadium atom can be described as a distorted octahedral with the tridentate hydrazone ligand coordinated in a meridional fashion, forming five- and six-membered chelate rings with bite angles of 74.8(2)° and 84.0(2)°, respectively, typical for this type of ligand systems [20]. The chelating hydrazone ligand lies in a plane with one hydroxylato ligand which lies *trans* to the hydrazone imino N atom. One carbonyl atom of the benzohydroxamate ligand *trans* to the oxo group completes the distorted octahedral coordination sphere at a rather elongated distance of 2.244(6) Å, due to the *trans* influence of the oxo group. This is accompanied by a significant displacement of the vanadium atom from the plane defined by the four basal donor atoms towards the apical oxo oxygen atom by 0.287(2) Å. The coordinate bond lengths are comparable to those of complex **I**, and also agree well with reported vanadium complexes containing the enolate form of this ligand type [20–22]. In the crystal packing structure of the complex, the ethanol molecules are linked to the hydrazone ligands through intermolecular hydrogen bonds of O–H···O (O(5)–H(5) 0.82, H(5)···O(7)^{i} 1.85, O(5)···O(7)^{i} 2.655(8) Å, O(5)–H(5)···O(7)^{i} 169(8)°; symmetry code for ^{i} $1-x$, $1-y$, $1-z$) (Fig. 2b).

The hydrazone compound H_2L and the two complexes were screened for antibacterial activities against two Gram (+) bacterial strains (*Bacillus subtilis* and *Staphylococcus aureus*) and two Gram (–) bacterial strains (*Escherichia coli* and *Pseudomonas fluorescence*) by MTT method. The MIC (minimum inhibitory concentration, μg mL^{-1}) values of the compounds against four bacteria are listed in Table 3. Penicillin G was used as the standard drug. The hydrazone compound shows strong activity against *S. aureus*, medium activity against *B. subtilis* and *E. coli*, and weak activity against *P. fluorescence*. The two complexes have strong activity against *B. subtilis* and *S. aureus*, medium activity against *E. coli*, while no activity against *P. fluorescence*. In general, the activities of both complexes are similar except for *E. coli*. The free hydrazone ligand and complexes show no activity against two fungal strains *Candida albicans* and *Aspergillus niger*.

FUNDING

This work was financially supported by K.C. Wong Magna Fund in Ningbo University, Ningbo natural science fund (project no. 201701HJ-B01019) and Ningbo Education Research Project (project no. 2017YZD001).

Table 3. Antimicrobial activities of the compounds **I** and **II**

Minimum inhibitory concentrations, μg mL^{-1}				
Tested material	*B. subtilis*	*S. aureus*	*E. coli*	*P. fluorescence*
H_2L	9.4	4.7	37.5	75
I	4.7	4.7	37.5	>150
II	4.7	4.7	75	>150
Penicillin G	2.3	4.7	>150	>150

REFERENCES

1. Kaplancikli, Z.A., Altintop, M.D., Ozdemir, A., et al., *Lett. Drug Des. Discov*., 2014, vol. 11, no. 3, p. 355.
2. Narisetty, R., Chandrasekhar, K.B., Mohanty, S., et al., *Lett. Drug Des. Discov.*, 2013, vol. 10, no. 7, p. 620.
3. Zhi, F., Shao, N., Wang, Q., et al., *J. Struct. Chem.*, 2013, vol. 54, no. 1, p. 148.
4. Ozdemir, A., Turan-Zitouni, G., Kaplancikli, Z.A., et al., *J. Enzyme Inhib. Med. Chem.*, 2008, vol. 23, no. 2, p. 470.
5. Loncle, C., Brunel, J.M., Vidal, N., et al., *Eur. J. Med. Chem.*, 2004, vol. 39, no. 12, p. 1067.
6. Liu, Y.-C., Wang, H.-L., Tang, S.-F., et al., *Anticancer Res.*, 2014, vol. 34, no. 10, p. 6034.
7. Krishnamoorthy, P., Sathyadevi, P., Cowley, A.H., et al., *Eur. J. Med. Chem.*, 2011, vol. 46, no. 8, p. 3376.
8. Zhang, M., Xian, D.-M., Li, H.-H., et al., *Aust. J. Chem.*, 2012, vol. 65, no. 4, p. 343.
9. Shi, L., Ge, H.-M., Tan, S.-H., et al., *Eur. J. Med. Chem.*, 2007, vol. 42, no. 4, p. 558.
10. Rai, N.P., Narayanaswamy, V.K., Govender, T., et al., *Eur. J. Med. Chem.*, 2010, vol. 45, no. 6, p. 2677.
11. Wazalwar, S.S., Bhave, N.S., Dikundwar, A.G., et al., *Synth. React. Inorg. Met.-Org. Nano-Met. Chem.*, 2011, vol. 41, no. 5, p. 459.
12. Liu, J.-L., Sun, M.-H., and Ma, J.-J., *Synth. React. Inorg. Met.-Org. Nano-Met. Chem.*, 2015, vol. 45, no. 1, p. 117.
13. Chohan, Z.H., Sumrra, S.H., Youssoufi, M.H., et al., *Eur. J. Med. Chem.*, 2010, vol. 45, no. 7, p. 2739.
14. Taheri, O., Behzad, M., Ghaffari, A., et al., *Transition Met. Chem.*, 2014, vol. 39, no. 2, p. 253.
15. SMART (version 5.625) and SAINT (version 6.01), Madison: Bruker AXS Inc., 2007.
16. Sheldrick, G.M., *SADABS, Program for Empirical Absorption Correction of Area Detector*, Göttingen: Univ. of Göttingen, 1996.
17. Sheldrick, G.M., *SHELXTL, Version 5.1, Software Reference Manual*, Madison: Bruker AXS, Inc., 1997.
18. Meletiadis, J., Meis, J.F.G.M., Mouton, J.W., et al., *J. Clin. Microbiol.*, 2000, vol. 38, no. 8, p. 2949.
19. Sarkar, A. and Pal, S., *Polyhedron*, 2007, vol. 26, no. 6, p. 1205.
20. Monfared, H.H., Alavi, S., Bikas, R., et al., *Polyhedron*, 2010, vol. 29, no. 18, p. 3355.
21. Zhang, X.-T., Zhan, X.-P., Wu, D.-M., et al., *Chin. J. Struct. Chem*., 2002, vol. 21, no. 7, p. 629.
22. Guo, S., Ding, Y., Li, A., et al., *Z. Anorg. Allg. Chem.*, 2018, vol. 644, no. 19, p. 1172.